Ionic Liquids Assisted Electrodeposition and Electrocatalytic Activity of PbO$_2$ electrodes

Lihua Yu, Juanqin Xue[*], *Yao Luo, Changbin Tang, Guoping Li*

School of Metallurgical Engineering, Xi'an University of Architecture and Technology, 13 Yanta Road, Xi'an 710055, PR China
[*]E-mail: huagong1985@163.com

PbO$_2$ coatings were electrodeposited on titanium substrates from solutions containing Pb(NO$_3$)$_2$ in the presence of an ionic liquid 1-ethyl-3-methyl-imidazolium tetrafluoroborate ([Emim]BF$_4$) by anodic oxidation technique. Influences of [Emim]BF$_4$ concentration and bath temperature on crystalline structure and electrocatalytic activity of resulting PbO$_2$ deposits were investigated by scanning electron microscopy (SEM), X-ray diffraction (XRD) and electrochemical oxidation of phenol simulated wastewater, respectively. A highly textured crystalline structure of β-PbO$_2$ with (110) plane being preferred orientation peak was obtained in the presence of [Emim]BF$_4$. An increase in [Emim]BF$_4$ concentration resulted in a higher degree of crystallinity and improved electrocatalytic activity of resulting deposits. Moreover, the crystalline structure of PbO$_2$ coatings was also greatly affected by bath temperature. The ratio of α-PbO$_2$/β-PbO$_2$ phases decreased with the increase in bath temperature. The preferential crystallographic orientation for β-PbO$_2$ in the (110) direction became more pronounced at higher temperatures. PbO$_2$ coatings with the optimum electrocatalytic activity were obtained in the presence of 50 mg·L^{-1} [Emim]BF$_4$ at 50℃. The activity of PbO$_2$ electrodes was found to be strongly dependent on their phase composition, degree of crystallinity and crystallite orientation.

1. INTRODUCTION

Nowadays, electrochemical oxidation has been studied intensively as a feasible and promising alternative technology for partial or total degradation of organic compounds which are toxic or resistant to biological treatment [1, 2]. The main advantages as often stressed in the literatures are versatility, energy efficiency, amenability to automation and cost effectiveness [3, 4]. The key factor for the application of electrochemical degradation with high current efficiency is electrode materials.

High stability, high activity and low cost are the desirable properties of electrodes [3, 5]. Various electrode materials, such as Pt [5-7], BDD [8, 9], PbO_2 [1-3, 5-7, 10, 11], SnO_2 [12, 13], and RuO_2 [4, 5, 14] have been developed and applied in mineralization of organic pollutants. Among these materials PbO_2 has been regarded as one of the promising anodic materials owing to its well-proven advantages, including good electrical conductivity, high oxygen evolution overpotential, high chemical stability in corrosive media, low cost, etc [1-3,10,11,15,16]. Usually, PbO_2 electrodes are prepared by electrochemically coating onto titanium substrates from aqueous electrolyte containing Pb(Ⅱ). The electrochemical behavior of electrodeposited PbO_2 is found to be very sensitive to the preparation method [1, 15]. As a result, PbO_2 coatings with different phase structures and a wide range of surface morphological characteristics can be prepared by the control of the electrodeposition parameters [1]. It has been proved that some amounts of foreign ions, surfactants, polyelectrolytes or oxides as additives to the deposition electrolyte can cause changes in electrodeposition kinetics, physico-chemical properties and electrocatalytic activity of resulting oxides [15-18]. For instance, R. Amadelli and coworkers found that the presence of bismuth ions in the electrodeposition solution caused a decrease in rate constants of PbO_2 formation due to Bi^{3+} ions adsorption on the electrode. Bi-doped deposits showed good adhesion to metal support and smaller size of crystal particles [15]. Likewise, a number of soluble organic additives, such as sodium lauryl sulphate, sodium dodecyl sulphonate (SDS), gelatin, dextrin, Triton X-100 and polyvinylpyrrolidone (PVP), have been used to interfere with the kinetics of PbO_2 electrodeposition and enhance the properties of PbO_2 coatings [17, 18]. Therefore, PbO_2 modification is one of the most promising ways of tailoring its solid state properties as well as its electrocatalytic activity [15].

Ionic liquids are liquids comprised entirely of cation-anion pairs with a melting temperature below 100℃. The unique properties of ionic liquids involve high charge density, thermal and electrochemical stability, a wide electrochemical potential window and low volatility [19]. The employment of ionic liquids either as electrolyte or as additive in the electrodeposition of metals and alloys has attracted intensive interest at present [20-22]. It is suggested that ionic liquids could change the properties of "electrode/electrolyte" interface and interfere with the electrodeposition process through adsorption on the electrode surface [20, 21]. However, the influence of ionic liquids as additives on the electrosynthesis of metal oxides at anode has not been reported yet.

1-ethyl-3-methyl-imidazolium tetrafluoroborate ([Emim]BF_4) is air and water stable, ease of preparation, non-toxic and capable of adsorption on metallic surface due to the lone electron pairs in nitrogen atoms of imidazolium cation [23]. In this work, [Emim]BF_4 was applied as an additive to the deposition electrolyte solution of Pb(NO_3)$_2$. Its effects on the morphology, structure and electrocatalytic activity of resulting PbO_2 were investigated. The mechanism of [Emim]BF_4 actions was studied and discussed in this paper. In addition to examining the role of [Emim]BF_4, the influences of bath temperature on the electrochemical behavior of resulting oxides were also discussed. The aims of this work were to determine the optimum conditions for PbO_2 electrodeposition in the presence of [Emim]BF_4 and obtain a fundamental understanding of the relationship between the coating structure and catalytic activity.

2. EXPERIMENTAL METHODS

2.1 Materials

Titanium plates (99.5% purity, 2 mm thickness) were used as the substrate for PbO_2 coatings due to its good electrical conductivity, sufficient mechanical strength, electrochemical inertness and easy formation of a protective film on its surface [3]. The plates were all cut into 3 cm×3 cm with a nominal reaction area of 20 cm^2. A stainless steel plate with the same area as the titanium plate was used as a cathode in electrodeposition. All chemical reagents were analytical grade and were used as received without further purification. Solutions were prepared using deionized Milli-Q water. Ionic liquid [Emim]BF$_4$ with 99% purity was available commercially from Chengjie Chemicals Company (Shanghai, China).

2.2 Preparation of lead dioxide electrodes

The titanium plates were mechanically polished using abrasive papers of successively finer roughness (180, 400, 800, 1200 grit) until a mirror surface was obtained. Then they were cleaned by acetone in an ultrasonic bath for 30 min to remove sand particles. After that the plates were degreased in 10(wt) % NaOH at 80℃ for 60 min. Finally, these plates were etched by boiling 10(wt) % oxalic acid for 120 min to thoroughly remove TiO_2. A grey titanium substrate with irregularity surface was obtained and conserved in an aqueous solution of 1(wt) % oxalic acid.

Lead dioxides were galvanostatically deposited at a current density of 10 mA·cm^{-2} for 60 min using a single compartment cell. The electrolyte solutions were composed of 0.4 M Pb(NO$_3$)$_2$ and 0.3 M HNO$_3$. The obtained Ti/PbO$_2$ electrodes were rinsed with doubly distilled water and dried. The mass of titanium plate were measured before and after electrodeposition so as to obtain the mass of PbO$_2$ coatings. The current efficiencies for anodic deposition of PbO$_2$ were determined from the weight gain of the titanium electrode on passing 720 C of charge.

2.3 Electrochemical oxidation

The electrochemical oxidation experiments were carried out in a batch apparatus consisting of a DC power supply, a magnetic stirrer and a single-compartment glass reactor. The self-made PbO$_2$ electrodes were applied as the anode and stainless steel plates of the same size were applied as the cathode. The electrode couple was positioned vertically and parallel to each other with a gap of 3 cm. 150 mL of electrolysis solution containing 100 mg·L^{-1} phenol as model pollutant and 0.25 M Na$_2$SO$_4$ as supporting electrolyte was oxidized at a constant current density of 10 mA·cm^{-2} and ambient temperature. During the experiments, samples were drawn from the reactor at certain intervals and analysed.

2.4 Characterization and Analysis

X-ray diffraction (XRD) was used to study the phase composition and crystallinity of prepared samples on a Shimadzu XRD-7000 diffractometer with Cu Kα (λ=0.15418 nm) radiation. Surface morphology of samples was studied by using scanning electron microscopy (JSM-6390A).

The chemical oxygen demands (CODs) of the phenol aqueous solution were measured by the titrimetric method using dichromate as the oxidant in acidic solution at 180℃ for 2 h.

2.5 Electrochemical tests

The electrochemical tests were performed employing a model PARSTAT4000 potentiostat/galvanostat instrument (Ametek, USA). Measurements were performed in a conventional three-electrode cell. Titanium sheet was used as the working electrode. The counter electrode was a graphite rod. A saturated calomel electrode (SCE) was used as the reference electrode, which was in contact with the working electrode through a Luggin tip. The cyclic voltammetric experiments were performed at a scan rate of 20 mV·s^{-1} in aqueous solution containing 0.3 M HNO_3 and 0.1 M $Pb(NO_3)_2$ in the presence or absence of [Emim]BF_4, respectively.

3. RESULTS AND DISCUSSION

3.1 Kinetic of PbO$_2$ electrodeposition process

Nowadays, most PbO_2 active coatings are prepared from electrolyte containing Pb^{2+} ions by electrodeposition technique due to its easy control of thickness and morphology of coatings, low cost, easily maintainable equipment and environmentally friendly [24]. It is thought that the electrocrystallization process is a crucial step determining the structure and morphology, as well as the electrochemical performance of resulting PbO_2 deposits [17]. However, the exact electro-chemical steps leading from Pb^{2+} in aqueous solution to solid PbO_2 is still unclear. Velichenco et al [25, 26] proposed the mechanism which involved adsorbed OH· being a key intermediate as shown in following reaction formulas:

$$H_2O \rightarrow OH\cdot_{ads} + H^+ + e \qquad (1)$$
$$Pb^{2+} + OH\cdot_{ads} \rightarrow Pb(OH)^{2+} \qquad (2)$$
$$Pb(OH)^{2+} + H_2O \rightarrow Pb(OH)_2^{2+} + H^+ + e \qquad (3)$$
$$Pb(OH)_2^{2+} \rightarrow PbO_2 + 2H^+ \qquad (4)$$
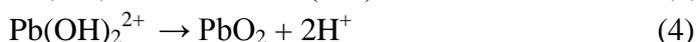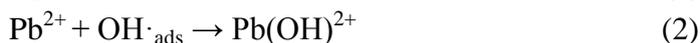
In order to achieve a preliminary understanding of the influence of [Emim]BF_4 on the kinetics of PbO_2 formation, the in-situ electrochemical tests were carried out.
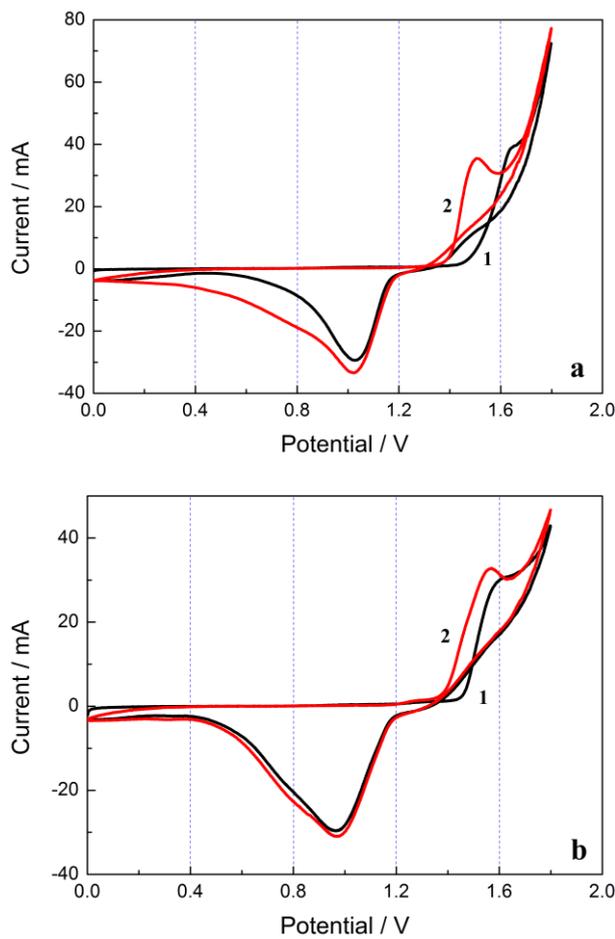
Figure 1. The cyclic voltammograms of electrochemical process carried out in $Pb(NO_3)_2$ and HNO_3 solution in the absence (a) and presence (b) of 50 mg·L^{-1} [Emim]BF_4 at a scan rate of 20 mV·s^{-1}

Fig. 1 shows the cyclic voltammograms of PbO_2 electrodeposition from electrolyte solutions in the absence (a) and presence (b) of 50 mg·L^{-1} [Emim]BF_4. At potentials around 1.4 V, a dramatic current growth corresponded to the reactions of Pb^{2+} oxidation. Then at potentials around 1.6 V, another sharp current rise can be attributed to the oxygen evolution [15], because some of the oxygen-containing species directly transferred to form oxygen and evolved away from the solution in the process of PbO_2 electrodeposition [17]. The initial oxygen evolution potential (OEP) in the presence of [Emim]BF_4 was apparently higher than that in the absence of [Emim]BF_4. Additionally, the current growth corresponding to oxygen evolution reaction in the presence of [Emim]BF_4 was significantly lower than that in the absence of [Emim]BF_4. The inhibition of oxygen evolution in the presence of [Emim]BF_4 may result from the adsorption of [Emim]BF_4 molecules on the electrode surface. The adsorbed layer was capable of inhibiting very active electrochemical sites which were responsible for production of the OH· radicals which were adsorbed intermediate for oxygen evolution [17, 18].

It can also be seen that the onset potential of PbO_2 deposition in the first cycle was more positive than that in the second cycle, indicating the further deposition of PbO_2 on the firstly deposited

PbO_2 layer was easier than that on bare titanium electrode. The results were in good agreement with the results reported by Shahram Ghasemi [18].

3.2 Effect of [Emim]BF_4 concentration

The influences of [Emim]BF_4 concentration on the current efficiency of deposition process were recorded and illustrated in Fig.2.
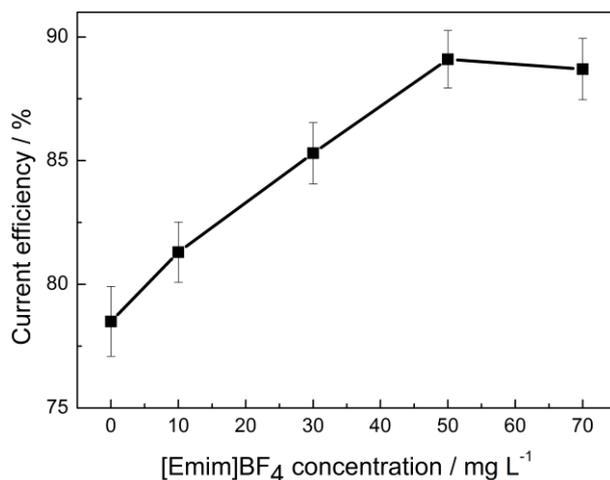
Figure 2. Effect of [Emim]BF_4 concentration on the current efficiency of PbO_2 electrodeposition on Ti substrate from solution containing 0.4 M $Pb(NO_3)_2$ and 0.3 M HNO_3 at 50℃

It can be seen that with the increasing of [Emim]BF_4 concentration from 0 mg·L^{-1} to 50 mg·L^{-1}, current efficiency rose from 78% to 89%. It may be attributed to the OEP rise in the presence of [Emim]BF_4 (Fig.1). It is well known that oxygen evolution contributes significantly to the total current thus decreasing the current efficiency of PbO_2 formation [17]. Therefore the higher OEP is helpful to restrain the side reaction of oxygen evolution and improve the current efficiency of PbO_2 electrosynthesis. As has been discussed previously, the inhibition of oxygen evolution in the presence of [Emim]BF_4 may be the result of its adsorption on the electrode surface. Therefore, the reason for the relatively stable current efficiency at concentration above 50 mg·L^{-1} may be that the surface adsorption had approached saturation at 50 mg·L^{-1}, consequently, the inhibition effects came to an end and more amount of addition was not helpful any more.

Fig.3 shows the XRD patterns of PbO_2 samples prepared in the absence and presence of different amount of [EMIM]BF_4. Parameters including peak wide and height at 25.4° and 49.1° are listed in Table 1. It can be seen that the tetragonal, rutile structure of lead dioxides (β-PbO_2) were mainly obtained from acid solutions, the amount of the orthorhombic α-form was rather small. Meanwhile, the β-PbO_2 deposits obtained in the presence of [EMIM]BF_4 were characterized by a preferential orientation in the (110) direction, indicating a highly textured structure of samples prepared in the presence of [EMIM]BF_4 [27]. Furthermore, the increase in concentration of

[EMIM]BF$_4$ was accompanied with a higher degree of crystallinity of the obtained PbO$_2$ samples, because X-ray diffraction patterns indicated an increase in peaks intensity with the increase in concentration of [EMIM]BF$_4$, whereas there was no obvious change in peak width of the diffraction lines (Table 1).
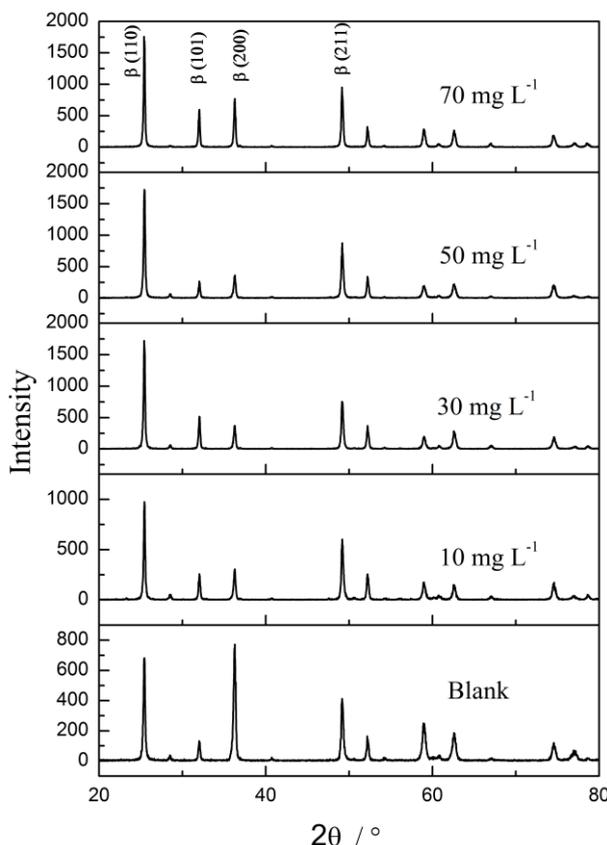
Figure 3. XRD spectrums of PbO$_2$ deposited from solution containing 0.4 M Pb(NO$_3$)$_2$ and 0.3 M HNO$_3$ in the presence of various concentrations of [Emim]BF$_4$ at 50℃

Table 1. The XRD data of PbO$_2$ deposited at different [EMIM]BF$_4$ concentrations

[EMIM]BF$_4$ concentration/ mg·L^{-1}	2θ=25.4º (β110)		2θ=49.1º (β211)	
	Wide	Height	Wide	Height
0	0.24	682	0.28	412
10	0.20	974	0.28	562
30	0.22	1720	0.28	754
50	0.22	1724	0.28	876
70	0.20	1756	0.26	950

SEM of PbO$_2$ films deposited in the absence and presence of 50 mg·L^{-1} [Emim]BF$_4$ at 50 ℃ are shown in Fig.4. Defects in the form of cracks and pores were observed for sample deposited in the absence of [Emim]BF$_4$. However, smooth surface, densely packed structure and a more regular

morphology was obtained in the presence of [Emim]BF$_4$. Meanwhile, the crystalline structure of modified PbO$_2$ was essentially enhanced with more pronounced edges and apexes. This observation was in agreement with the results of X-ray diffractograms.
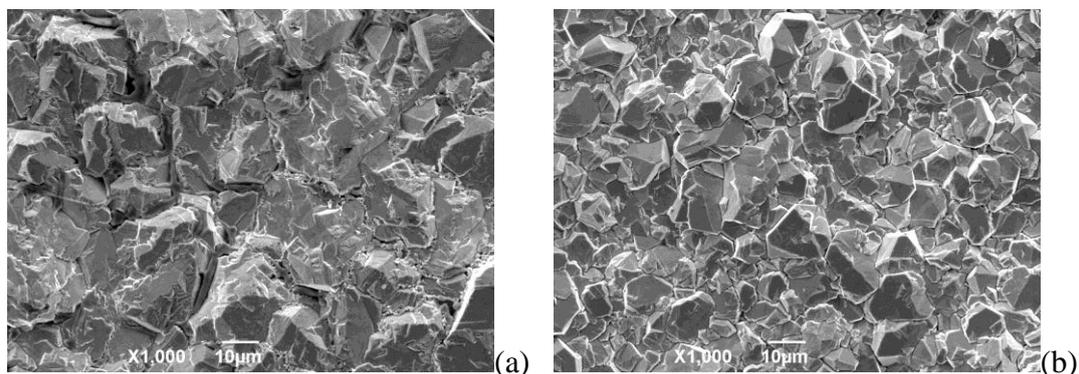
Figure 4. Scanning electron micrographs of PbO$_2$ deposited from solution containing 0.4 M Pb(NO$_3$)$_2$ and 0.3 M HNO$_3$ in the absence (a) and presence (b) of 50 mg·L^{-1} [Emim]BF$_4$ at 50℃
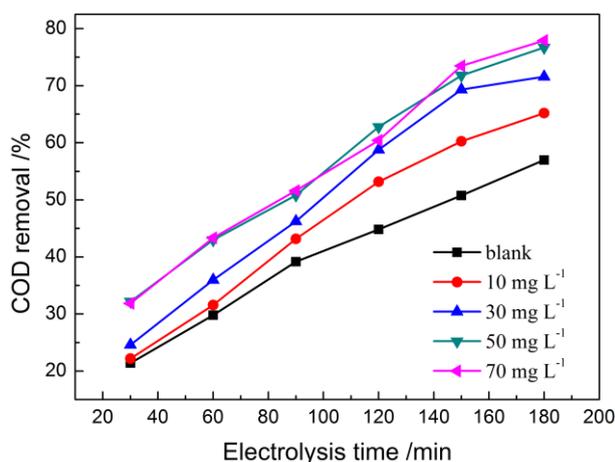
Figure 5. COD removal rate during electrolysis of 100 mg·L^{-1} phenol at a current density of 10 mA·cm^{-2} by PbO$_2$ electrodes deposited in the presence of various concentrations of [Emim]BF$_4$ at 50℃

Bulk electrolysis of 100 mg·L^{-1} phenol was performed to investigate the electrocatalytic activity of PbO$_2$ anodes at a current density of 10 mA·cm^{-2}. The results (Fig.5) indicated that the activities of anodes prepared in the presence of [Emim]BF$_4$ were obviously higher than that prepared in the absence of [Emim]BF$_4$. The increase of [Emim]BF$_4$ concentration in the deposition bath was accompanied with the improvement of the activity of resulting electrodes. In addition, electrodes prepared in the presence of < 30 mg·L^{-1} [Emim]BF$_4$ were observed to peel after a few uses, but anodes prepared in the presence of ≥30 mg·L^{-1} [Emim]BF$_4$ showed better adhesion to substrate and much longer service time. It could be related to the higher crystallinity of the PbO$_2$ deposits achieved in the presence of ≥30 mg·L^{-1} [Emim]BF$_4$. Because the more crystalline is the sample, the harder is its

adherence to Ti substrate [17]. It may also be attributed to the inhibition of oxygen evolution by [Emim]BF$_4$ in the process of PbO$_2$ electrodeposition. Because the formed oxygen may cause cracks in the oxide structure and this structural defects would eventually accelerate the failure of oxide coating during its application as anode at high potentials.

3.3 Effect of bath temperature

Electrolyte temperature is known to be an important parameter greatly determining the electro-crystallization behavior of metal oxides.
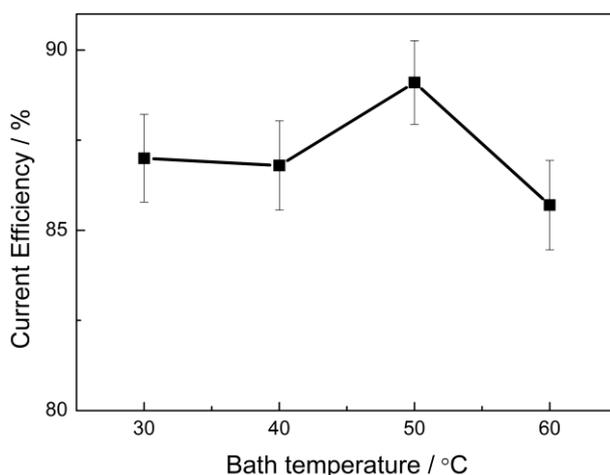
Figure 6. Effect of bath temperature on the current efficiency of PbO$_2$ electrodeposition on Ti substrate from solution containing 0.4 M Pb(NO$_3$)$_2$ and 0.3 M HNO$_3$ in the presence of 50 mg·L^{-1} [Emim]BF$_4$

It can be seen from Fig.6 that with the increase of bath temperature from 30℃ to 60℃, current efficiency for the production of PbO$_2$ coatings fluctuated from 85% to 89%. The influence of bath temperature on the current efficiency of deposition process was relatively mild compared with that of [Emim]BF$_4$ concentration. The temperature influences all diffusion processes such as ion diffusion in the electrolyte and surface diffusion of the nuclei [28]. Elevated bath temperature provide higher diffusion rate of surface adatoms compared to the creation of hydroxyl radicals. Therefore, the oxygen evolution as well as the current efficiency of PbO$_2$ production was also affected by bath temperature. According to the results, the highest current efficiency was achieved at 50℃. The drop of current efficiency at 60 ℃ may be attributed to the sensitivity of [Emim]BF$_4$ adsorption to high temperature.

The crystalline structure and phase composition of the prepared electrodes was studied by XRD as a function of bath temperature. From the X-ray diffraction patterns shown in Fig.7, it can be seen that preferential crystallographic orientation for β-PbO$_2$ in the (110) direction became more pronounced at higher temperatures of 40℃ and 50℃ than that at 30℃. The results indicated that an increase of the temperature favored the formation of better defined PbO$_2$ crystals. It's worth noting that

peak corresponding to (200) plane became the strongest one when bath temperature rose to 60℃. The preferential crystallographic orientation of crystals is thought to be related to the selective adsorption of additives on electrode surface. Therefore, the shift in preferential orientation may be attributed to the variation of adsorption behavior of [Emim]BF$_4$ on electrode surface at temperature as high as 60℃.
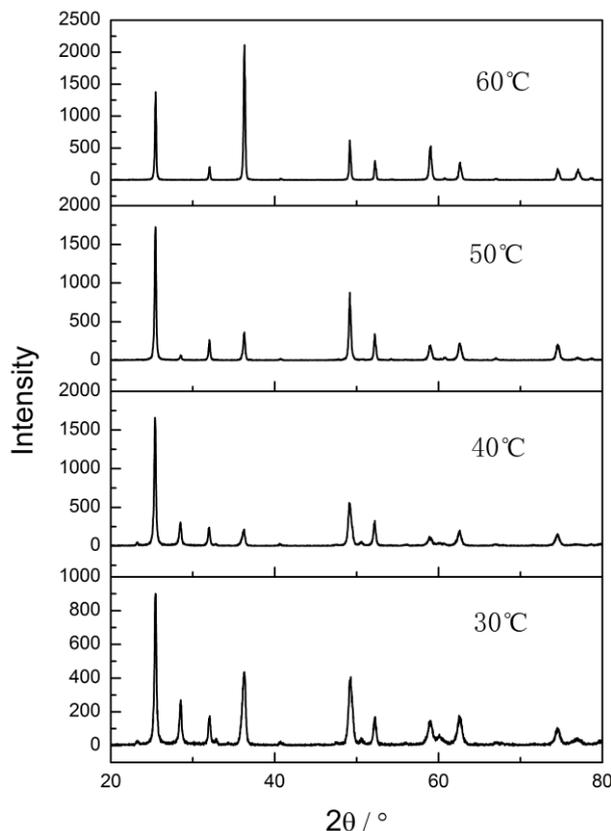
Figure 7. XRD spectrums of PbO$_2$ deposited at various bath temperatures from solution containing 0.4 M Pb(NO$_3$)$_2$ and 0.3 M HNO$_3$ in the presence of 50 mg·L^{-1} [Emim]BF$_4$

Both forms of PbO$_2$ (α-PbO$_2$, β-PbO$_2$) were found in samples deposited at 30℃. With an increase in bath temperature, the intensities of the β-PbO$_2$ peaks became more intense whereas the intensities of the α-PbO$_2$ peaks were diminished. Only β-PbO$_2$ presented in samples prepared at 60℃. The percentage of the α form (W$_\alpha$) in the mixtures of the two phases was calculated using the following relation proposed by Munichandraiah [29]:

$$\frac{2J_\alpha}{J_{\beta 1} + J_{\beta 2}} = KW_\alpha$$

Where J$_\alpha$ is the relative intensity of the (111) plane of α-PbO$_2$, J$_{\beta 1}$ and J$_{\beta 2}$ are the relative intensities of the (110) and (101) planes of β-PbO$_2$ respectively. The proportionality constant (K) was calculated using the XRD peak intensities of a known mixture of α and β-modifications of the PbO$_2$. Using the value of K (equal to 0.0139 per wt %), the percentage of the α-modification present in the PbO$_2$ coating was calculated and shown in Table 2. It can be seen that the content of α-phase sharply decreased with increased bath temperature, indicating that the ratio of α/β forms strongly depended on the bath temperature. This result was in good agreement with literature reports [1, 24, 27, 30-32]. For

example, pure α-PbO$_2$ was formed at 25 ℃ and pure β-PbO$_2$ at 75 ℃ with both forms deposited at intermediate temperatures when deposition was carried out from 0.5 M Pb(CH$_3$SO$_3$)$_2$ + 0.5 M CH$_3$SO$_3$H onto vitreous carbon [30]. It is possible that during the rise in bath temperature, the mass transport increases. Consequently, recrystallization to the more stable β-PbO$_2$ takes place from the metastable α-PbO$_2$ [24, 31].

Table 2. The XRD data of PbO$_2$ deposited at different bath temperatures

Temperature/℃	2θ/radians	Height	Relative intensity/%	W_{α}	h k l index α-PbO$_2$	β-PbO$_2$
30	25.4	900	100.0		-	1 1 0
	28.5	270	30.0		1 1 1	-
	32.0	176	19.6	36	-	1 0 1
	36.2	432	48.0		-	2 0 0
	49.1	380	42.2		-	2 1 1
40	25.4	1658	100.0		-	1 1 0
	28.5	306	18.5		1 1 1	-
	32.0	240	14.5	23	-	1 0 1
	36.2	200	12.1		-	2 0 0
	49.1	558	33.7		-	2 1 1
50	25.4	1724	100.0			1 1 0
	28.5	68	3.9		1 1 1	-
	32.0	266	15.4	5	-	1 0 1
	36.2	362	21.0		-	2 0 0
	49.1	876	50.8		-	2 1 1
60	25.4	1378	65.3		-	1 1 0
	32.0	208	9.9	0	-	1 0 1
	36.2	2110	100.0		-	2 0 0
	49.1	622	29.5		-	2 1 1

Fig.8 presents the scanning electron micrographs of different PbO$_2$ samples deposited in the presence of [Emim]BF$_4$ at 30℃ and 50℃ respectively. There were remarkable differences between the microstructural features of the two samples. Sample prepared at 30℃ exhibited a higher degree of surface roughness and irregularity. However, sample prepared at 50℃ showed a relatively smoother, regular morphology and densely packed structure.

It can be seen from Fig.9 that temperature had a significant effect on the electrocatalytic activity of PbO$_2$ anodes towards organic pollutants degradation. Much higher COD removal rates were achieved for the electrodes deposited at 50℃ than that deposited at 30℃ and 40℃. It can be attributed to the rapid decrease in the content of α-phase impurities and more pronounced preferential crystallographic orientation in the (110) direction of β phase at 50℃. Because it has been well proven that β-PbO$_2$ possessed much higher performance than α-PbO$_2$ on phenol degradation due to their

conductivity and structure differences [33]. In addition, better defined crystals were thought to possess relative higher activity [32, 33].
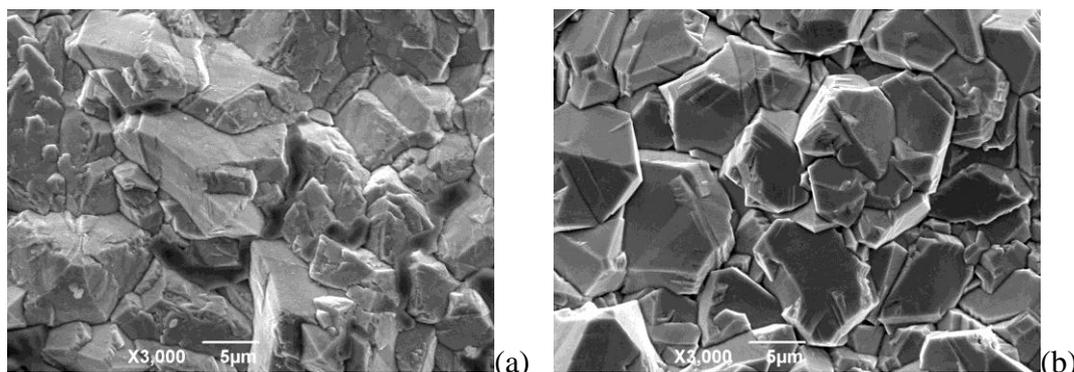
Figure 8. Scanning electron micrographs of PbO_2 deposited at (a)30℃ (b)50℃ from solution containing 0.4 M $Pb(NO_3)_2$ and 0.3 M HNO_3 in the presence of 50 mg·L^{-1} [Emim]BF_4
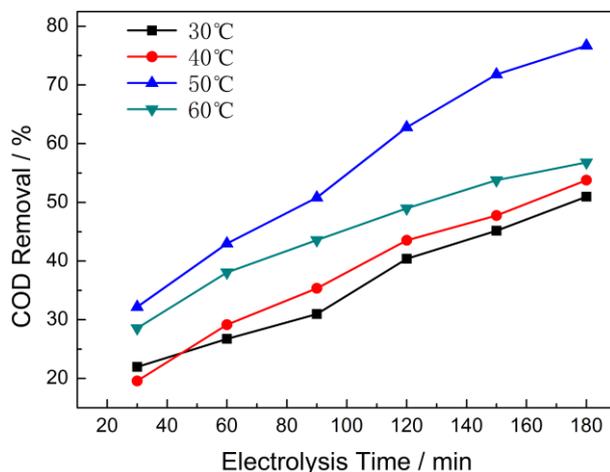
Figure 9. COD removal rate during electrolysis of 100 mg·L^{-1} phenol at a current density of 10 mA·cm^{-2} by PbO_2 electrodes deposited at various temperatures

The further increase in bath temperature from 50 ℃ to 60 ℃, however, resulted in a decrease in the COD removal rate of resulting deposits. This might be caused by the change of preferential crystallographic orientation for β-PbO_2 from (110) plane at 50℃ to (200) plane at 60℃. It has been known that some crystals employed in photocatalytic processes had their unique shape and facet-dependent activities due to the differences in surface energies between different planes [34-36]. For instance, the (111) faces of Cu_2O nanostructure were catalytically more active than the (100) faces because the (111) face contained surface copper atoms with dangling bonds and interacted more strongly with methyl orange [34, 35]. Similarly, the results in this work demonstrated that β-PbO_2 with preferential orientation along (110) plane possessed higher electrocatalytic capacity on phenol degradation than that with preferential orientation along (200) plane. However, the underlying reason remains open to investigation.

All the data together proved the importance of the PbO_2 electrode phase structure, including crystallinity, phase composition and preferential orientation, on its electrocatalytic activity at the incineration of organic pollutants. However, far more efforts should be done to draw definitive conclusions about the correlation between deposits type and electrochemical performances.

4. CONCLUSIONS

The conclusions drawn from the work described here are as follows:

1)   The addition of [Emim]BF_4 to electrodeposition solution resulted in the inhibition of oxygen evolution reaction, which favored the higher current efficiency for PbO_2 formation and more adhesion of PbO_2 coating to Ti substrate.

2)   The structural, compositional and morphological properties of resulting PbO_2 coatings were strongly influenced by [Emim]BF_4 modification. PbO_2 coatings with compact and regular morphology and a highly textured structure were obtained on Ti substrate when [Emim]BF_4 was present in the deposition electrolyte. The increase in [Emim]BF_4 concentration resulted in a higher degree of crystallinity of PbO_2.

3)   The ratio of α-PbO_2/β-PbO_2 forms decreased with the increase in bath temperature. Besides, preferential crystallographic orientation for β-PbO_2 in the (110) direction became more pronounced at higher temperatures of 40℃ and 50℃. However, the preferential orientation of β-PbO_2 shifted to (200) plane when bath temperature reached up to 60℃.

4)   Both [Emim]BF_4 modification and bath temperature markedly affected the activity of resulting PbO_2 deposits towards phenol degradation. PbO_2 coatings with the optimum activity were obtained in the presence of 50 mg·L^{-1} [Emim]BF_4 at 50℃. The electrocatalytic activity of PbO_2 electrodes was strongly dependent on its phase structure. β-PbO_2 showed higher electrocatalytic activity than α-PbO_2, and higher degree of crystallinity increased the electrocatalytic activity of pure β-PbO_2. In addition, crystallite orientation of β-PbO_2 deposits also had a marked influence on their electrocatalytic activity.

References

1. X. H. Li, D. Pletcher, F. C. Walsh, *Chem. Soc. Rev.,* 40 (2011) 3879.
2. C. Sáez, P. Cañizares, J. Llanos, M. A. Rodrigo, *Electrocatalysis,* 4 (2013) 252.
3. G. H. Chen, *Sep.Purif. Techno.,* 38 (2004) 11.
4. M. Li, C. P. Feng, W. W. Hu, Z. Y. Zhang, N. Sugiura, *J. Hazard Mater.,* 162 (2009) 455.
5. Y. J. Feng, X. Y. Li, *Water Res.*, 37 (2003) 2399.
6. C. A. Martinez-Huitle, S. Ferro, A. De Battisti, *Electrochim. Acta,* 49 (2004) 4027.

7. Y. M. Tang, C. M. Kong, *Mater. Chem. Phys*., 135 (2012) 1108.
8. M. Murugananthan, S. Yoshihara, T. Rakuma, T. Shirakashi, *J. Hazard Mater.,* 154 (2008) 213.
9. J. F. Zhi, H. B. Wang, T. Nakashima, T. N. Rao, A. Fujishima, *J. Phys. Chem. B*, 107 (2003) 13389.
10. Y. Liu, H. L. Liu, *Electrochim. Acta,* 53 (2008) 5077.
11. Y. Liu, H. L. Liu, J. Ma, J. J. Li, *Electrochim. Acta,* 56 (2011) 1352.
12. Y. J. Feng, Y. H. Cui, J. F. Liu, B. E. Logana, *J. Hazard Mater*., 178 (2010) 29.
13. Y. H. Cui, Y. J. Feng, Z. Q. Liu, *Electrochim. Acta,* 54 (2009) 4903.
14. M. Panizza, G. Cerisola, *Environ. Sci. Technol*., 38 (2004) 5470.
15. O. Shmychkova, T. Luk'yanenko, A. Velichenko, L. Meda, R. Amadelli, *Electrochim. Acta,* 111 (2013) 332.
16. R. Amadelli, L. Armelao, A. B. Velichenko, N. V. Nikolenko, D. V. Girenko, S. V. Kovalyov, F. I. Danilov, *Electrochim. Acta,* 45 (1999) 713.
17. M. Ghaemi, E. Ghafouri, J. Neshati, *J. Power Sources,* 157 (2006) 550.
18. S. Ghasemi, M. F. Mousavi, M. Shamsipur, *Electrochimica Acta,* 53 (2007) 459.
19. J. A. Latham, P. C. Howlett, D. R. MacFarlane, M. Forsyth, *Electrochem. Commun*., 19 (2012) 90.
20. S. H. Wang, X. W. Guo, H. Y. Yang, J. C. Dai, R. Y. Zhu, J. Gong, L. M. Peng, W. J. Ding, *Appl. Surf. Sci.,* 288 (2014) 530.
21. Q. B. Zhang, Y. X. Hua, *J. Appl. Electrochem*., 39 (2009) 261.
22. Q.B. Zhang, Y.X. Hua, *J. Appl. Electrochem*., 41 (2011) 481.
23. X. Zhou, H. Y. Yang, F. H. Wang, *Electrochim. Acta,* 56 (2011) 4268.
24. T. Mahalingam, S.Velumani, M. Raja, S.Thanikaikarasan, J. P. Chu, S. F. Wang, Y. D. Kim, *Mater. Charact*., 58 (2007) 817.
25. A. B. Velichenko, D. V. Girenko, F. I. Danilov, *Electrochim. Acta*, 40 (1995) 2803.
26. A. B. Velichenko, R. Amadelli, E. A. Baranova, D. V. Girenko, F. I. Danilov, *J. Electroanal. Chem*., 527 (2002) 56.
27. H. An, Q. Li, D. J. Tao, H. Cui, X. T. Xu, L. Ding, L. Sun, J. P. Zhai, *Appl. Surf. Sci*., 258 (2011) 218.
28. H. Natter, R. Hempelmann, *Electrochim. Acta,* 49 (2003) 51.
29. N. Munichandraiah, *J. Appl. Electrochem*., 22 (1992) 825.
30. I. Sires, C. T. J. Low, C. Ponce de Leon, F. C. Walsh, *Electrochim. Acta,* 55 (2010) 2163.
31. S. Abaci, K. Pekmez, T. Hokelek, A. Yildiz, *J. Power Sources,* 88 (2000) 232.
32. A. B. Velichenko, R. Amadelli, A. Benedetti, D. V. Girenko, S. V. Kovalyov, F. I. Danilov, *J Electrochem Soc.,* 149 (2002) C445.
33. S. Abaci, U. Tamer, K. Pekmez, A. Yildiz, *Appl. Surf. Sci*., 240 (2005) 112.
34. J. Y. Ho, M. H. Huang, *J. Phys. Chem. C,* 113 (2009) 14159.
35. C. H. Kuo, M. H. Huang, *J. Phys. Chem. C,* 112 (2008) 18355.
36. C. H. Kuo, M. H. Huang, *Nano Today,* 5 (2010) 106.